Terahertz imaging of composite materials in reflection and transmission mode with a time-domain spectroscopy system

Trygve R. Sørgård, Arthur D. van Rheenen, and Magnus W. Haakestad

Norwegian Defence Research Establishment (FFI), P O Box 25, NO-2027 Kjeller, Norway

ABSTRACT

A fiber-coupled Terahertz time domain spectroscopy (THz-TDS) system based on photoconductive antennas, pumped by a 100-fs fiber laser, has been used to characterize materials in transmission and reflection mode. THz images are acquired by mounting the samples under investigation on an x–y stage, which is stepped through the beam while the transmitted or reflected THz waveform is captured. The samples include a carbon fiber epoxy composite and a sandwich-structured composite panel with an aramid fiber honeycomb core in between two skin layers of fiberglass reinforced plastic. The former has an artificially induced void, and from a comparison of recorded reflected time-domain signals, with and without the void, a simple model for the structure of the composite is proposed that describes the time-domain signals reasonably well.

Keywords: Terahertz, imaging, composites, non-destructive testing

1. INTRODUCTION

Non-destructive testing (NDT) refers to methods for inspection of materials or structures without permanently altering the inspected objects. NDT is important within quality control during manufacturing, but also for inspection of materials or components on a regular basis to look for damage. Several techniques for performing NDT exist, including ultrasound, thermography, X-rays, and TV holography. Recently, Terahertz technology has emerged as a promising technology for performing NDT.[1–6] Examples of applications of THz technology within NDT include inspection of car paint layers[7] and inspection of coating thickness for pharmaceutical tablets.[8]

One especially interesting application of NDT with THz waves is within analysis of composite materials.[9] This type of materials can be engineered to be both stronger and lighter than traditional materials, such as metals, and they are therefore useful in for example aircrafts, body armor, automotive components, buildings, and sports equipment. In this work, a fiber-coupled THz-TDS system is used to characterize two different composite materials in transmission and reflection mode. The materials under investigation include a sandwich-structured composite panel with an aramid fiber honeycomb core in between two skin layers of fiberglass reinforced plastic (fiberglass composite) and a carbon fiber epoxy composite (carbon fiber composite). We take advantage of the fact that both the amplitude and phase of the transmitted or reflected Terahertz pulses are measured when characterizing the materials. In transmission mode, the propagation delay and transmission spectrum in each pixel provides useful information regarding the samples. In reflection mode, the measured THz waveform provides information regarding the structure of layered materials, and deconvolution of the time-domain data helps interpreting the measurements.

2. SETUP

The THz setup is based on time-domain spectroscopy with fiber-coupled photoconductive antennas,[10] and is schematically shown in Fig. 1. The photoconductive antennas are driven by 100-fs pulses at 780 nm wavelength from a frequency-doubled Er-doped fiber laser. THz images are acquired by mounting the composite samples on an x–y stage, which is scanned through the beam, with step size 1 mm, while the transmitted or reflected THz waveform is captured. Normal incidence onto the samples is used in transmission mode, while the angle of incidence is approximately 15° in reflection mode, with horizontal polarization of the THz beam. Careful

Further author information: (Send correspondence to M.W.H.)
M.W.H.: E-mail: Magnus-W.Haakestad@ffi.no, Telephone: +47 6380 7263

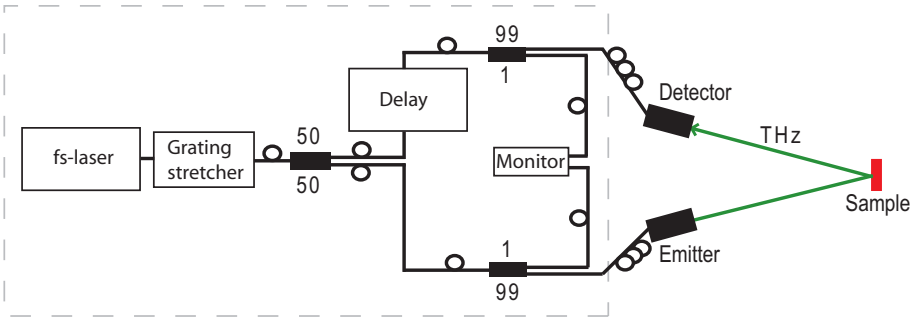

Figure 1. A schematic of the fiber-coupled THz-TDS setup when used in reflection mode.

alignment of the samples is needed in reflection mode, because only the specular reflection is detectable. The propagation distance from the emitter to the detector module is approximately 31 cm and the measurements are carried out in ambient air (21–26°C, 10–50% relative humidity). The signal at each position of the x–y stage (pixel) is measured with a sampling rate of 32 Hz, a time window of 80–300 ps, and a scan speed of 1–10 ps/s.

3. SAMPLES

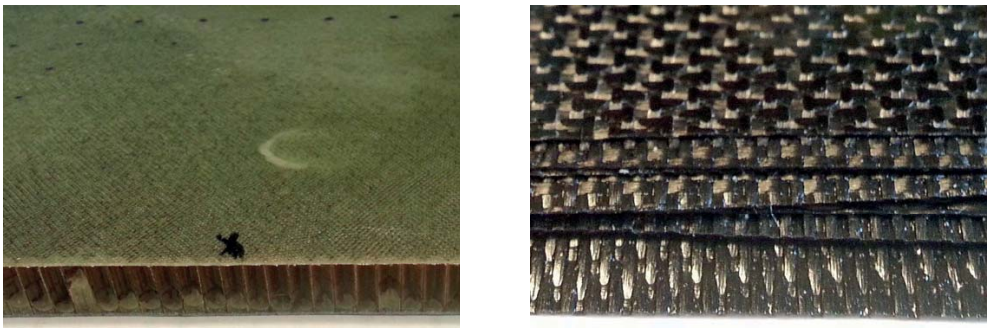

Figure 2. Images of the two composite samples under investigation. (a) sandwich-structured composite panel, (b) carbon fiber epoxy composite.

We characterize two different composite samples. The first sample is a sandwich-structured composite panel, with a total thickness of 14 mm. An image of this material is shown in Fig. 2(a). It has two skin layers of fiberglass reinforced plastic, each with a thickness of 1 mm. The core material is a honey comb structure, with thickness 12 mm, consisting of plascore aramid fiber. The diameter of each honey comb cell is 5 mm. The sample is hit by a hammer in an attempt to cause damage. The hammer impact can be seen to the right of the center in Fig. 2(a). This composite material is used in a radome (a structural, weatherproof enclosure that protects a radar system).

The second material is a carbon fiber epoxy composite. An image of this sample is shown in Fig. 2(b). It consists of 11 layers of carbon fibers (Toray M30SC) which are pre-impregnated with epoxy. The composite is made by heating and pressing together the 11 impregnated layers. Each layer is rotated by 90° with respect to the neighboring layers. A defect in the composite is made by removing a 2 cm × 2 cm square from the central layer. The total thickness of the sample is 3.2 mm, corresponding to a thickness of 0.29 mm for a single layer. This composite is used in pressure vessels.

4. SIGNAL PROCESSING

Measurements are carried out in transmission and reflection mode. In THz-TDS the transmitted or reflected electric field amplitude as a function of time, $y(t)$, is acquired. The task is to determine the structure of the sample (refractive index as a function of position and frequency), but this inverse scattering procedure is impossible in general.[11] Retrieving the structural parameters of the sample thus requires extra information about the material under investigation. If such information is not available, it is useful instead to plot the measured data in a way such that it may be interpreted by a human operator. We found that the peak delay of the THz pulses can provide some information about the samples. The peak delay is easily obtained from $y(t)$, also for highly absorbing samples. In addition, plotting the energy content of the transmitted or reflected pulses in a certain frequency range, e.g. from 0.5–1 THz, can provide some additional information.

In reflection mode, it is in addition useful to perform some more advanced signal processing than just plotting the peak delay and energy content of the pulses. The more advanced data processing used here is as follows: The measured signal $y(t)$ is multiplied by a window function, $b(t)$, giving $y_w(t) = y(t)b(t - t_0)$, where t_0 is the time of the peak amplitude. We here use a Blackman-Harris asymmetric window function, with 7 ps (start) and 40 ps (end) half widths. The Fourier transform, $\hat{y}_w(\nu) = \mathrm{FFT}(y_w)$, is then calculated. The reflection coefficient is determined by dividing $\hat{y}_w$ by a reference measurement (transmission through air), $\hat{z}_w(\nu)$, giving $\hat{r}(\nu) = \hat{y}_w(\nu)/\hat{z}_w(\nu)$. The calculated reflection coefficient only gives meaningful values in the frequency region where the signal-to-noise ratio is high. We therefore multiply the reflection coefficient by a bandpass filter,[12,13] $\hat{w}_r(\nu) = \hat{r}(\nu)\hat{w}(\nu)$, where $\hat{w}(\nu) = \mathrm{FFT}[w(t)]$ and

$$w(t) = f_H e^{-(f_H t)^2} - f_L e^{-(f_L t)^2}. \quad (1)$$

The coefficients $f_L = 0.5$ THz and $f_H = 3.0$ THz are used here, which can be considered as low-frequency and high-frequency cut-offs for the filter. The inverse Fourier transform of $\hat{w}_r(\nu)$ is then calculated, giving $w_r(t)$. We can consider $w_r(t)$ as the reflected signal when the incident THz pulse is given by $w(t)$. The advantage of this deconvolution process is that the input waveform illuminating the sample may have a complicated pulse shape and deconvolution is equivalent to calculating the reflected waveform for a simple input pulse, given by $w(t)$. This process may thus help identifying the layers in the sample, as we show below. The different steps of the deconvolution process are shown in Fig. 3 for a reflection measurement of the carbon fiber composite.

5. RESULTS

5.1 Sandwich-structured composite panel

Figure 4 shows measured data for the glass fiber composite. A 6 cm × 6 cm square of this composite was imaged. A hammer was used to make a dent to the composite, as shown in Fig. 4(a). A metal tape along the border of the imaged region was used for reference purpose. The peak delay for the reflected pulse from the front surface of the composite is shown in Fig. 4(b). We observe from the figure that the extra peak delay in the position of the hammer mark is about 0.2 ps, corresponding to a position shift of 30 μm. Also, the hammer mark changes the reflection coefficient of the front surface, as observed in Fig. 4(c). An image of the transmitted energy in the frequency range 0–0.5 THz (with the metal tape removed) is shown in Fig. 4(d), where the honeycomb structure of the composite core is apparent. However, a clear interpretation of the picture is difficult. The peak delay in transmission did not provide any useful information for this sample. Also, reflections from layers other than the front surface of the composite were difficult to interpret.

5.2 Carbon fiber epoxy composite

5.2.1 Transmission

Measurements on the carbon fiber composite in transmission mode are shown in Fig. 5. The carbon fiber composite transmitted about 1% of the incident energy, and the transmission was practically zero above 0.6 THz. The defect in the central layer is readily apparent in the plot of the peak delay in Fig. 5(a), because of the reduction of 0.85 ps for the propagation time through the defect (missing layer). The defect also affects the transmitted energy, as shown in Fig. 5(b), but the defect is not as clear in this image, compared to the plot of the peak delay.

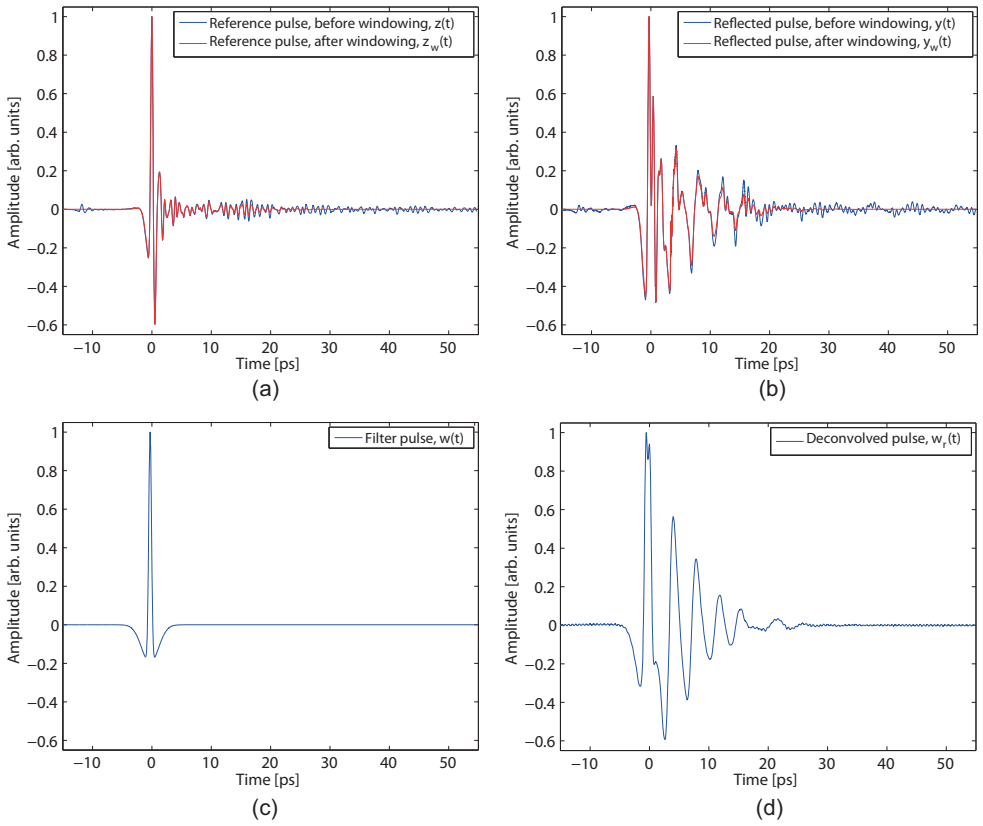

Figure 3. Illustration of the deconvolution procedure. (a) Reference pulse (without sample), (b) reflected pulse from composite, (c) filter pulse, $w(t)$, (d) deconvolved pulse, $w_r(t)$.

5.2.2 Reflection

While the transmitted waveform gives information about the average properties of the sample under investigation, more detailed information is potentially available in reflection mode. In Fig. 6, we plot the results from a so-called B-scan (line scan) through the defect. Figure 6(a) and (b) shows the raw data from this scan on a linear scale and logarithmic scale, respectively. Although some of the layer structure of the sample is apparent in these plots, it is difficult to identify the defect. By using the deconvolution procedure described in Sec. 4, we plot the resulting data in Fig. 6(c) and (d) on a linear and logarithmic scale, respectively. The defect in the middle layer (layer no. 6 from the top) is readily observed in the logarithmic plot.

6. MODEL

We can model the reflection properties of the carbon fiber composite using some simple considerations. First, all the 11 sheets are assumed to have identical properties. Second no anisotropy is assumed, because the reflected signal is quite similar when the sample is rotated by 90°. Third, each sheet is assumed to be symmetric, i.e. the properties are identical when illuminated from the front side and the back side, because this was observed experimentally. Finally, the refractive indexes are assumed to be independent of frequency. The simplest model taking these points into account is a three-layer model, where each of the 11 sheets can be considered as a a slab of thickness d_1 and refractive index n_1, surrounded on each side by a layer with thickness d_2 and refractive index n_2. The total thickness of a single sheet is thus $d_s = d_1 + 2d_2$. Experimentally, we have $d_s = 0.29$ mm.

Figure 7 shows two reflected signals from the carbon fiber composite (from the defect and beside the defect, respectively). The signals are obtained from the measurements using deconvolution. Also shown is an estimate

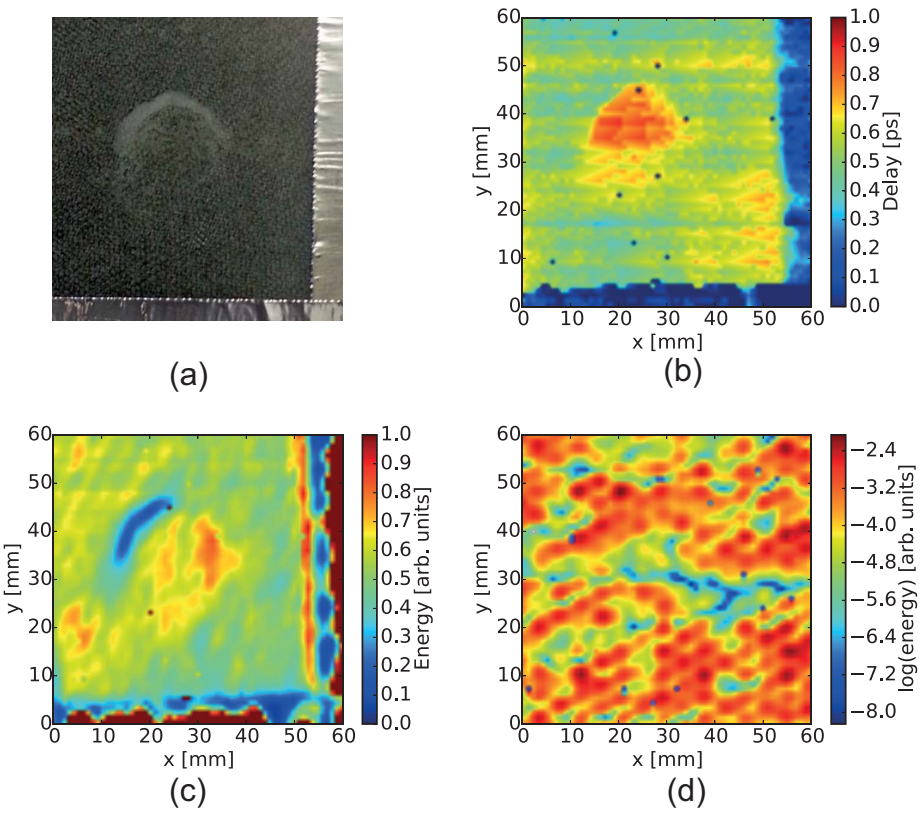

Figure 4. Measurements on sandwich-structured composite panel. (a) Visual image, (b) Peak delay in reflection mode, (c) reflected energy, (d) transmitted energy in frequency range 0–0.5 THz (log scale).

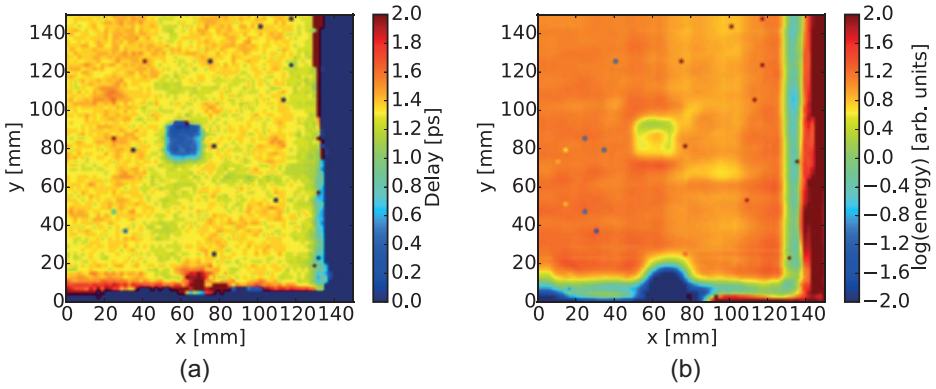

Figure 5. Measurements on carbon fiber epoxy composite in transmission mode. (a) Peak delay, (b) transmitted energy in frequency range 0-0.5 THz (log scale).

of the refractive index profile, based on the three-layer model of each sheet. The estimated refractive index profile is based on the fact that a step up in refractive index corresponds to a positive peak and a step down in refractive index corresponds to a negative peak in the reflected signal. Measured delay in reflection from two neighboring sheets is $2t_s = 3.81$ ps. This gives a transit time of $t_s = 1.91$ ps through a single sheet, which is equivalent to an optical thickness of $d_{o,s} = 0.57$ mm, which again is equivalent to an effective refractive index

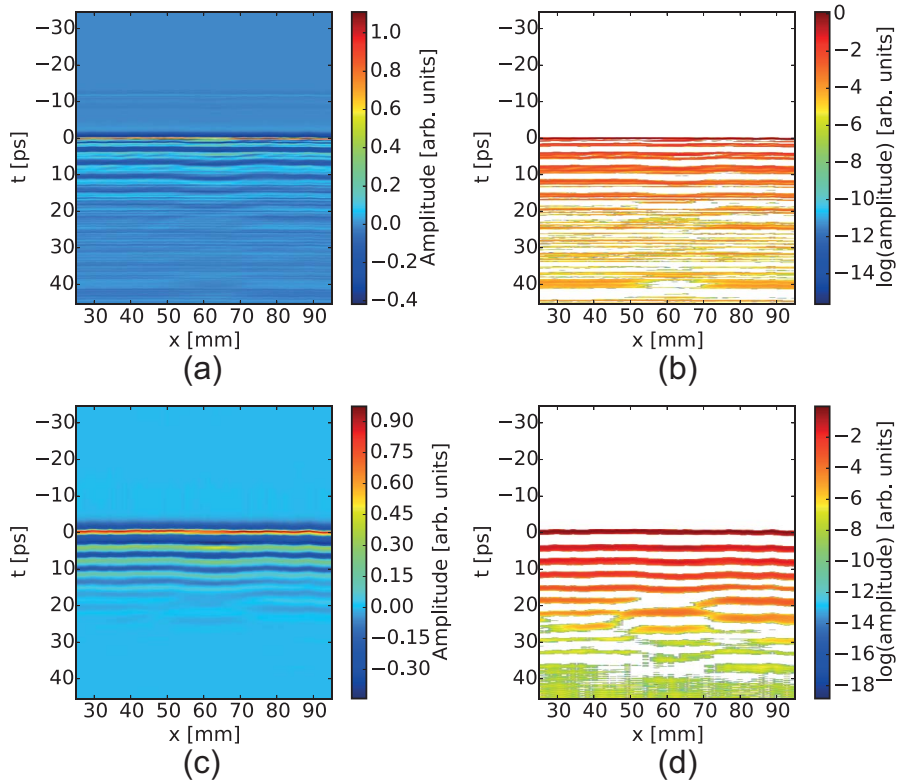

Figure 6. Line scan along the defect for the carbon fiber epoxy composite in reflection mode. (a) raw data, (b) raw data, log scale, (c) deconvolved signal, (d) deconvolved signal, log scale.

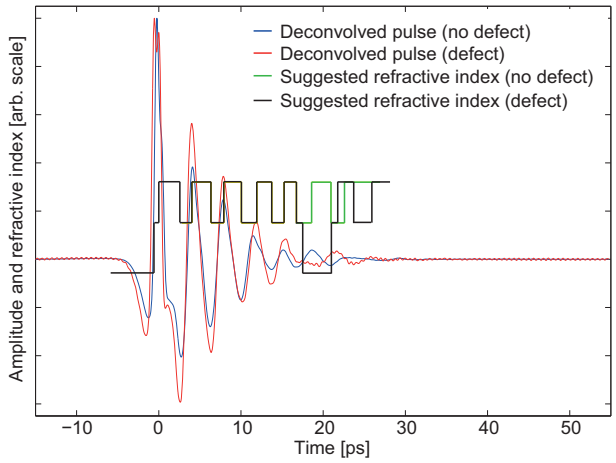

Figure 7. Measurement on carbon fiber composite in reflection. The figure shows a measured reflected pulse profile beside the defect (blue) and at the defect (red). Also shown is a modeled refractive index profile beside the defect (green) and at the defect (black).

of $n_{\text{eff}} = d_{o,s}/d_s = 1.97$ for a single sheet. Furthermore, we find that the time separation from a positive peak to a negative peak in the reflected signal is $2t_1 = 2.09$ ps, while the time separation from a negative peak to a positive peak in the reflected signal is $4t_2 = 1.72$ ps. We can thus conclude that the propagation time through a high index layer, with thickness d_1, is $t_1 = 1.05$ ps, corresponding to an optical thickness of $d_{o,1} = 0.32$ mm,

while the propagation time through one low index layer, with thickness d_2, is $t_2 = 0.43$ ps, corresponding to an optical thickness of $d_{o,2} = 0.13$ mm. This information is not sufficient to determine d_1, d_2, n_1, and n_2, but once one of these quantities is known, the remaining quantities are determined.

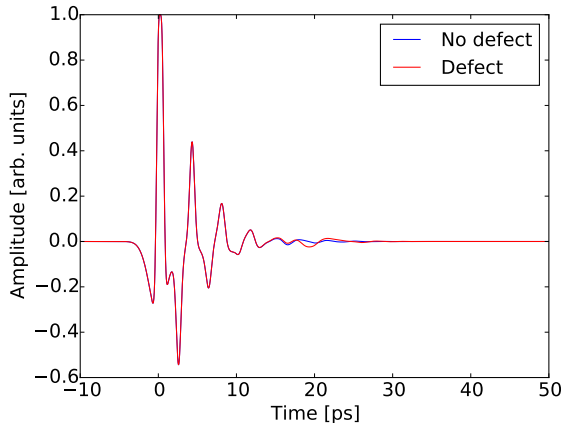

Figure 8. Modeled response of carbon fiber composite in reflection. The figure shows a simulated reflected pulse profile beside the defect (blue) and at the defect (red).

Using the transfer-matrix method,[11] one can calculate the reflected pulses from the carbon fiber composite. The defect is assumed to be due to a missing central sheet. Using the parameters above, we vary the thickness d_1. In addition, loss is taken into account by adding an imaginary part to the refractive index n_1. By optimizing these two parameters to match the calculated pulses to the measured pulses, we obtain the pulses shown in Fig. 8. The following parameters are used in this model: d_1 =0.128 mm, d_2 =0.081 mm, $n_1 = 2.50 + 0.25i$, and n_2 =1.60. In addition, we assume a thickness of 0.041 mm, instead of 0.081 mm, for the very first layer, in order to get a reasonable agreement between the model and the simulation. The model reproduces many of the features in Fig. 7 reasonably well, despite its simplicity. However, a refined model, where dispersion of n_1 and n_2 is taken into account, would most likely be needed to get an even better correspondence between measured and simulated pulses.

We then consider the central layer in each sheet and wish to estimate its electrical conductivity. Assuming that the current density is proportional to the electric field, $\mathbf{J} = \sigma\mathbf{E}$, where σ is the electrical conductivity, and using the Maxwell equation $\nabla \times \mathbf{H} = \mathbf{J} - i\omega\epsilon\mathbf{E} = -i\omega\left(\epsilon + i\sigma/\omega\right)\mathbf{E}$, where $\epsilon = \epsilon_r\epsilon_0$ is the dielectric permittivity, we can define an effective refractive index $n = \sqrt{\epsilon_r + i\sigma/(\omega\epsilon_0)}$. By using the value of n_1 obtained above, and assuming a frequency $\omega/(2\pi)$ =0.5 THz, we estimate an effective electrical conductivity of $\sigma = 35$ S/m in the central layer. While the electrical conductivity of carbon fiber composites may vary by orders of magnitude,[14] this value is within the reported range.

7. CONCLUSIONS

A glass fiber composite and a carbon fiber composite has been imaged using a THz-TDS system in reflection and transmission mode. The peak delay and transmitted energy provides useful information, especially in transmission mode. Deconvolution of the signal in reflection mode helps identifying defects in a layered carbon fiber composite. Based on the time-domain measurements in reflection mode and some simple approximations, a structural model for the carbon-fiber based composite could be constructed, that fits the main features of the measured traces reasonably well.

ACKNOWLEDGMENTS

We thank Tom Thorvaldsen and Torbjørn Olsen for providing the composite samples.

REFERENCES

1. Tonouchi, M., "Cutting-edge terahertz technology," *Nature Photonics* **1**, 97–105 (Feb. 2007).
2. Chan, W. L., Deibel, J., and Mittleman, D. M., "Imaging with terahertz radiation," *Rep. Prog. Phys.* **70**, 1325–1379 (July 2007).
3. Redo-Sanchez, A., Karpowicz, N., Xu, J., and Zhang, X.-C., "Damage and defect inspection with terahertz waves," in [*The 4th International Workshop on Ultrasonic and Advanced Methods for Nondestructive Testing and Material Characterization*], (June 2006).
4. Palka, N., Krimi, S., Ospald, F., Miedzinska, D., Gieleta, R., Malek, M., and Beigang, R., "Precise determination of thicknesses of multilayer polyethylene composite materials by terahertz time-domain spectroscopy," *J Infrared Milli Terahz Waves* **36**, 578–596 (2015).
5. Jördens, C., Scheller, M., Wietzke, S., Romeike, D., Jansen, C., Zentgraf, T., Wiesauer, K., Reisecker, V., and Koch, M., "Terahertz spectroscopy to study the orientation of glass fibres in reinforced plastics," *Composites Science and Technology* **70**, 472–477 (2010).
6. Zhang, J., Shi, C., Ma, Y., Han, X., Li, W., Chang, T., Wei, D., Du, C., and Cui, H.-L., "Spectroscopic study of terahertz reflection and transmisssion properties of carbon-fiber-reinforced plastic composites," *Optical Engineering* **54** (May 2015). Paper no. 054106.
7. Su, K., Shen, Y.-C., and Zeitler, J. A., "Terahertz sensor for non-contact thickness and quality measurement of automobile paints of varying complexity," *IEEE Transactions on Terahertz Science and Technology* **4**, 432–439 (July 2014).
8. Fitzgerald, A. J., Cole, B. E., and Taday, P. F., "Nondestructive analysis of tablet coating thickness using terahertz pulsed imaging," *Journal of Pharmaceutical Sciences* **94**, 177–183 (Jan. 2005).
9. Stoik, C. D., Bohn, M. J., and Blackshire, J. L., "Nondestructive evaluation of aircraft composites using transmissive terahertz time domain spectroscopy," *Optics Express* **16**, 17039–17051 (Oct. 2008).
10. Ellrich, F., Weinland, T., Theuer, M., Jonuscheit, J., and Beigang, R., "Fiber-coupled Terahertz spectroscopy system," *Techn. Messen* **75**, 14–22 (2008).
11. Skaar, J. and Haakestad, M. W., "Inverse scattering of dispersive stratified structures," *J. Opt. Soc. Am. B* **29**, 2438–2445 (Sept. 2012).
12. Chen, Y., Huang, S., and Pickwell-MacPherson, E., "Frequency-wavelet domain deconvolution for terahertz reflection imaging and spectroscopy," *Optics Express* **18**, 1177–1190 (Jan. 2010).
13. Palka, N., Panowicz, R., Ospald, F., and Beigang, R., "3d non-destructive imaging of punctures in polyethylene composite armor by THz time domain spectroscopy," *J Infrared Milli Terahz Waves* **36**, 770788 (2015).
14. Piche, A., Revel, I., and Peres, G., "Experimental and numerical methods to characterize electrical behaviour of carbon fiber composites used in aeronautic industry," in [*Advances in Composite Materials - Analysis of Natural and Man-Made Materials*], Tesinova, P., ed., InTech (2011).